

# Assessing SAR Calibration Requirements Using Geophysical Retrieval Algorithms

## Executive Summary

JT Macklin, PA Wright and A Pilgrim (BAE SYSTEMS), T Le Toan and A Bouvet (CESBIO), and NP Walker (eOsphere)

---

### EUROPEAN SPACE AGENCY CONTRACT REPORT

The work described in this report was done under ESA contract.

Responsibility for the contents resides in the author or organisation that prepared it.

---

TES 105585 / February 2010



# Assessing SAR Calibration Requirements Using Geophysical Retrieval Algorithms Executive Summary

TES 105585 - 1.0  
February 2010

Prepared by  
JT Macklin, PA Wright and A Pilgrim (BAE SYSTEMS), T Le Toan and A Bouvet  
(CESBIO), and NP Walker (eOsphere)

## SIGNATURES

Author:	_____	Trevor Macklin	
Approved by:	_____	Trevor Macklin	Project Manager
Approved by:	_____	Vaughan Stanger	Group Leader
Authorised by:	_____	John Milsom	Head of Department

BAE SYSTEMS Advanced Technology Centre  
West Hanningfield Road, Great Baddow, Chelmsford, Essex CM2 8HN

THIS DOCUMENT WAS PRODUCED UNDER THE TERMS AND CONDITIONS OF CONTRACT  
20729/06/NL/HE FOR DR. N. FLOURY, EUROPEAN SPACE RESEARCH AND TECHNOLOGY  
CENTRE, THE NETHERLANDS.

The copyright in this document is vested in the study team, comprising BAE SYSTEMS, CESBIO and eOsphere Limited. This document may only be reproduced in whole or in part, or stored in a retrieval system, or transmitted in any form, or by any means electronic, mechanical, photocopying or otherwise, either with the prior permission of BAE SYSTEMS or in accordance with the terms of ESTEC Contract No. 20729/07/NL/HE.

**DOCUMENT INFORMATION:**

Project No: 111060	Local Document Ref.: GSY/090322/111060
Project Title: ESA geophysical calibration	

**CHANGES SINCE LAST ISSUE:**

None

**DISTRIBUTION****Full**

Copy No	Name	Company
1 - 3	Dr. N. Flourey	ESA (ESTEC)
4	Library	Baddow/Filton
5	Dr. P. Woods	ATC
6	Mr. J. Milsom	ATC
7	Dr. T. Le Toan	CESBIO
8	Mr. N. Walker	eOsphere Ltd
9	Dr. J.T. Macklin	ATC

**Abstract only**

A1	Mr. A. Levenston	ATC (electronic format)
A2	Dr. M. Worboys	ATC (electronic format)

<b>ESA STUDY CONTRACT REPORT</b>			
<b>ESA CONTRACT N° 20729/07/NL/HE</b>		<b>SUBJECT Assessing SAR Calibration Requirements Using Geophysical Retrieval Algorithms</b>	
		<b>CONTRACTOR BAE SYSTEMS (UK)</b>	
<b>ESA CR( ) No</b>	<b>STAR CODE</b>	<b>No of volumes : 2 This is Volume No : 2</b>	<b>CONTRACTOR'S REFERENCE TES 105585</b>
<b>ABSTRACT :</b>			
<p>This is the Executive Summary for the Final Report on Contract 20729/07/NL/HE for ESA ESTEC on "Assessing SAR Calibration Requirements Using Geophysical Retrieval Algorithms". The overall objective of this study is to develop performance models and trade-off plots which link the accuracies of geophysical parameters retrieved from synthetic-aperture radar (SAR) data to the values of key SAR system parameters. The study covers four main technical tasks:</p> <p>WP 10: review and state of the art</p> <p>WP 20: theoretical assessment of SAR system parameter impact for six applications, namely ocean wind speed, generic segmentation, rice monitoring, forest biomass density, sea-ice classification and sea-ice lead detection</p> <p>WP 30: practical assessment of SAR system parameter impact using SAR images for these applications</p> <p>WP 40: conclusions and recommendations.</p>			
The work described in this report was done under ESA Contract. Responsibility for the contents resides in the author or organisation that prepared it.			
<b>Names of authors :</b> <b>J T Macklin, P A Wright and A Pilgrim (BAE SYSTEMS), T Le Toan and A Bouvet (CESBIO) and N P Walker (eOsphere Limited)</b>			
<b>NAME OF ESA STUDY MANAGER Nicolas Flourey (TEC-EEP)</b>		<b>ESA BUDGET HEADING</b>	
<b>DIV: Electromagnetics and Space Environments (EE)</b>		<b>060 - GSP</b>	
<b>DIRECTORATE: TEC</b>			

## **Introduction**

This is the Executive Summary for the Final Report on Contract 20729/07/NL/HE for ESA ESTEC on “Assessing SAR Calibration Requirements Using Geophysical Retrieval Algorithms”. The overall objective of this study is to develop performance models and trade-off plots which link the accuracies of geophysical parameters retrieved from synthetic-aperture radar (SAR) data to the values of key SAR system parameters. The study covers four main technical tasks:

WP 10: review and state of the art

WP 20: theoretical assessment of SAR system parameter impact

WP 30: practical assessment of SAR system parameter impact using SAR images

WP 40: conclusions and recommendations.

SAR parameters need to be optimised to suit the retrieval accuracies demanded by science and applications. Calibration accuracy affects the ability to merge data and assimilate with models, as well as the generation of reliable, long-term series of data. The present study allows all of these aspects to be addressed.

The study begins with a survey of the properties of spaceborne SAR systems, their impact on the accuracy of geophysical retrieval algorithms and the present status of applications of interest to this project. Spaceborne SAR systems offer or plan to offer radar frequencies from P to Ku band, and various instrument modes (polarimetry, spatial resolutions down to 1 m, and swaths up to about 500 km). Thermal noise levels are typically in the range -20 dB to -25 dB, while radiometric stability or accuracy is typically in the range 0.5 – 1 dB.

In generic terms, the SAR image quality parameters affect products in the following ways:

- Radiometric retrievals from the magnitude and/or phase of the observed backscatter (e.g. forest biomass densities and ocean wind fields). The most important factors are expected to include: the radiometric resolution, stability and accuracy, thermal noise, ambiguities from other distributed targets, and cross-talk and channel imbalance.
- Spatial products, where the accurate location of features is important (e.g. ship tracking and mapping). Here the most important factors are expected to be the spatial resolution, sidelobes and ambiguities.
- Combined radiometric and spatial products (e.g. land-use and sea-ice maps). All of the factors mentioned under the previous two headings are potentially important here.

The following applications were selected for further study:

- Ocean wind speed and direction
- Generic segmentation in order to understand the ability to distinguish regions of different size and contrast
- Rice monitoring
- The estimation of forest biomass density from low-frequency SAR data
- The classification of sea-ice types
- The detection of leads in sea-ice.

The results for each application are now discussed in turn.

**Ocean Wind**

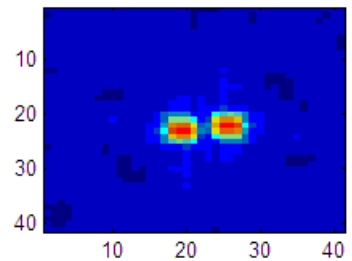
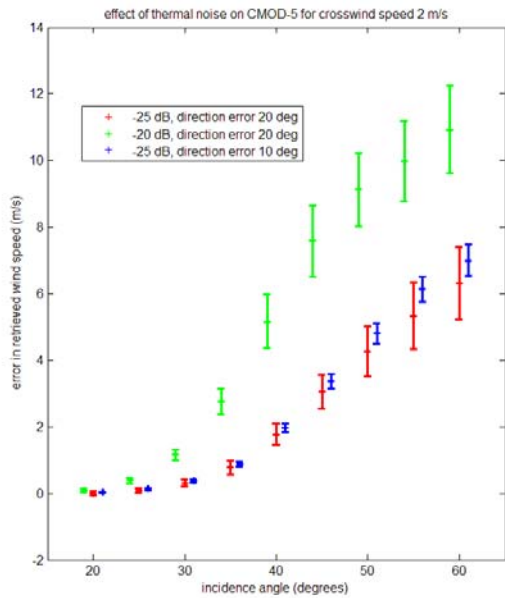
The user requirements set limits on both the lowest and highest incidence angles which may be used to retrieve wind speeds to a given accuracy. The upper limit is set by the levels of thermal noise and ambiguities which may be tolerated. The lower limit is set by the sensitivity of the backscattering coefficient to changes in wind speed.

The combined effects of systematic errors in the backscattering coefficient and random errors in the wind direction are assessed by Monte Carlo simulation. Figure 1 (left) shows the results for different levels of thermal noise added to a true crosswind speed of 2 m s<sup>-1</sup>. Such plots enable the highest incidence angle to be estimated which satisfies a given accuracy in the retrieved wind speed. The modelling developed here allows the user to explore the impact of changing parameters such as the assumed accuracies, range of wind speeds, thermal noise and ambiguity level.

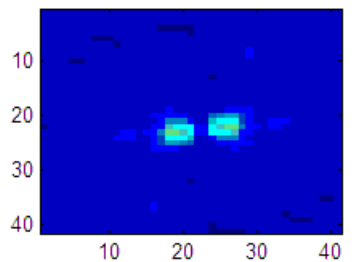
Ocean wind retrievals from SAR data are not limited by speckle, because of the amount of spatial averaging required to smooth over the variations from ocean waves. The analysis of actual image data has established the following behaviour in deep-water sites:

- Spatial variability has negligible effect on accuracy of the retrieved wind speed on scales from 1 – 15 km.
- Fourier analysis shows that there is negligible error in estimates of wind direction from wind streaks even when high thermal noise is added to SAR images (Figure 1, right).

A more detailed investigation would be needed to establish the behaviour in coastal waters, where finer spatial resolution is likely to be needed to resolve effects arising from aspects such as limited fetch and local topography. A key question to address is: how close to the coast can wind speeds be derived from SAR data, given a user requirement on accuracy?



*no thermal noise added*



*noise equal to mean signal added*

**Figure 1 Left: effects of thermal noise and errors in wind direction on retrieved wind speed for a crosswind of 2 m/s (C band, vertical polarisation). Right: example power spectra of wind streak signatures: the axes are pixel numbers.**

**Generic Segmentation**

Segmentation is an important step in many retrieval and classification processes, but it can be difficult to assess the accuracy of the results on actual data. Here, simple performance measures are established and applied to a simulated image. The simulation is a chequerboard where the numbers of tiles, their sizes, their backscatter values and the number of looks are all chosen by the user. The user may add thermal noise or an ambiguous region to the scene.

The radiometric performance measure is the Student t-statistic, defined by:

$$t = \frac{(\sigma_1 - \sigma_2)}{\sqrt{V_1 + V_2}} \tag{1}$$

where  $\sigma$  and  $V$  are the mean and the variance in the mean, respectively, for each region. Possible measures for the spatial performance include the number of pixels in a region, the length of the region perimeter, and the location errors in the horizontal and vertical directions.

The analysis may be applied to any segmentation algorithm. Figure 2 (left) shows the dependence of the t-statistic for segmentations of 10 x 10 pixel tiles with  $\sigma_1 = -11.8$  dB,  $\sigma_2 = -17.3$  dB, three-look speckle, and different thermal noise levels. As the noise increases, the segmentation is progressively worse. Plots may also be produced to show the effect of the differences between the segmented boundaries and their true positions.

Figure 2 (right) shows histograms of t-values for segmentations of two areas from a DLR ESAR image over Remningstorp forest in Sweden which is also used for the forest application here. Lower t-values occur when thermal noise is added to both areas. Area B is harder to segment due to saturation in the relationship between backscatter coefficient and biomass.

The ability to segment images can be understood in terms of a basic set of attributes (mean, standard deviation and number of independent pixels), provided an additional attribute is included to describe the texture in terms of the departure from the expected standard deviation from a speckled, uniform scene. The addition of thermal noise may also be expressed as an equivalent degradation of spatial resolution by computing the histogram of the ratio of t-values. This is useful because the required spatial resolution is often the most well established parameter for many applications. For Area A we find that the addition of -20 dB thermal noise is equivalent to a spatial resolution which is coarser by a factor of 1.16.

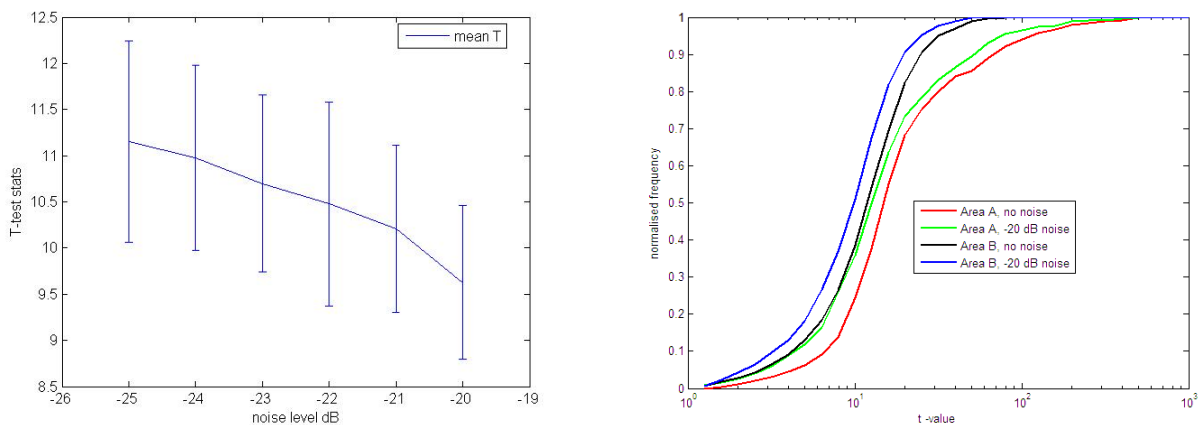


**Figure 2 Left: t-statistic as a function of thermal noise for the above example. Right: cumulative histogram of t-values for segmentations of two areas without and with -20 dB thermal noise.**



## Rice Monitoring

We assess the accuracy of pixel-based classification methods which use a decision rule based on a threshold intensity. Algorithms using the temporal change of the backscatter and the polarisation ratio are considered.

A theoretical error model is developed to express the probability of error (PE) in the classification as a function of four input parameters:

- $p(\mathbf{B})$  is the *a priori* probability of the rice class.
- $\Delta r$ , the “distance” between the mean ratios of the rice and non-rice classes
- $d$ , a bias between a measured ratio and the corresponding true ratio
- $\mathbf{ENL}$ , the equivalent number of looks in the images.

These parameters may then be linked to satellite system parameters, image processing parameters and scene parameters.

An empirical data model is introduced to represent the temporal behaviour of the backscattering characteristics of the rice and the non-rice classes during a whole rice growing cycle. The error model and the data model are used jointly to assess the impacts of satellite repeat cycle, ambiguity ratio, channel gain imbalance and radiometric stability. The duration of the satellite repeat cycle was found to be a critical parameter for the temporal change method, while it has a small effect in the polarisation ratio method. For the mapping of short cycle (<90 days) varieties, values such as 12 or 6 days (Sentinel-1 with 1 or 2 satellites) are indicated.

A data-set of Alternating Polarisation images from ASAR over a test site in the Mekong delta has been used in the study, with polarisations HH and VV in each image. The data are acquired every 35 days during one rice season, which allows only three acquisitions. A GIS land-cover dataset is used to estimate the additional error in the classification accuracy when degradations are introduced into the images. The effects of radiometric stability and channel gain imbalance are simulated by shifting the classification threshold, and the images need not be degraded.

The additional errors caused by channel gain imbalance in the polarisation ratio method and radiometric stability in the temporal change method agree well with the model, with absolute differences below 2.5% (Figure 3). The results therefore show that the model can be used effectively to assess the effects of channel imbalance, radiometric stability and ambiguity level.

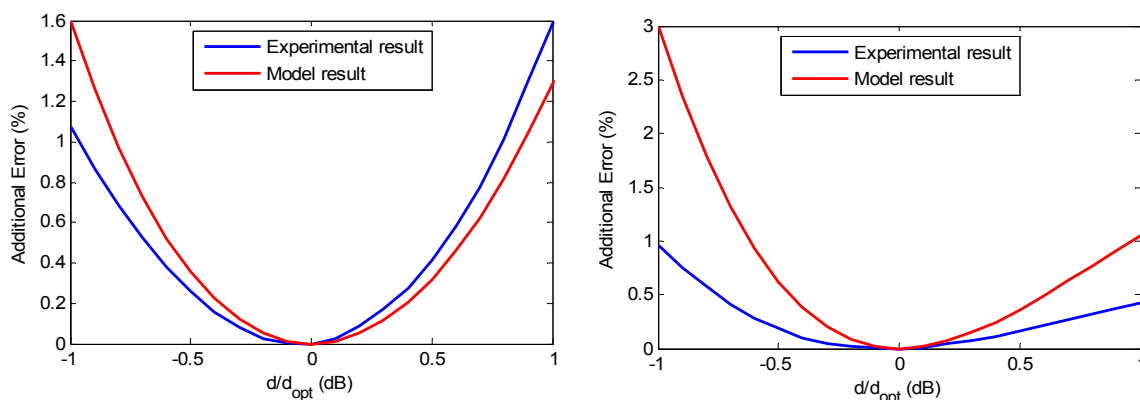


**Figure 3 Comparison of the experimental results (blue curves) and the model result (red curves) on the effect of parameter  $d$  on the additional classification error for the polarization ratio method (left) and for the temporal change method (right).**

**Forest Biomass Density**

An empirical model is used to assess the impact of two SAR system parameters on the biomass retrieval: radiometric stability and ambiguity ratio. Another SAR system parameter is discussed but not included in the theoretical assessment: the thermal noise. For a general and simple algorithm, P-HV is proposed for biomass inversion, based on an empirical relationship between P-HV intensity and forest above ground biomass.

The data set used to test the model is one P-band E-SAR image acquired in 2006 on a forest area located near Remningstorp, Sweden. A biomass map is produced from the image (after incidence angle normalisation and filtering) by applying the empirical relationship. This map is used as the reference to calculate the error due to image degradations. The general methodology consists of image degradation, followed by application of the biomass inversion equation, and comparison of the retrieved biomasses from the degraded and original images.

The simulations show that if the **radiometric stability**  $\Delta\gamma$  is  $< 0.3$  dB, the resulting error in biomass is small compared to the uncertainty due to speckle noise; for example the error due to radiometric stability is less than 10 ton/ha for biomass of 200 ton/ha. For an assumed achievable radiometric stability of 0.5 dB, the corresponding error in biomass will be about 25 ton/ha (12.5% of the biomass value). The errors derived from the data are in excellent agreement with the simulated results (Figure 4 left). High radiometric accuracy is required for biomass  $> 150$  ton/ha due to saturation in the relationship between biomass and backscatter coefficient. For example, at 300 ton/ha,  $\Delta\gamma_{HV}$  should be  $< 0.5$  dB to attain an error  $< 60$  ton/ha.

**Thermal noise** and **distributed ambiguities** affect low values of the backscatter. Low thermal noise (e.g.  $\leq -27$  dB) is required to have reduced error in biomass in the range of 1-10 ton/ha, to increase the frequency of regrowth monitoring during the lifetime of the satellite. For a typical -20 dB ambiguity level and a stand of 10 ton/ha adjacent to a stand of 300 ton/ha, the error in retrieved biomass is about 5 ton/ha, representing 50% of biomass (Figure 4, right).

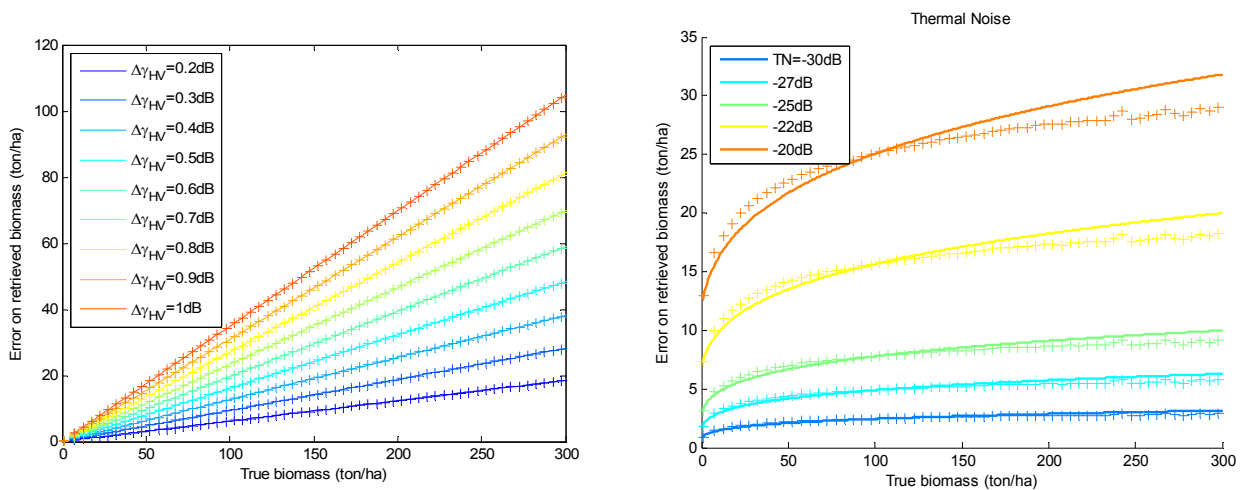


**Figure 4 Left: error in estimated biomass expressed as a function of biomass (in ton/ha) of the radiometric stability  $\Delta\gamma$ . The crosses are data values and the lines are theoretical predictions. Right: error in retrieved biomass for different levels of thermal noise (TN).**

### ***Sea-Ice Type Classification and Lead Detection***

A model has been set up to understand how SAR system parameters impact on quantitative measures of retrieval accuracy for certain sea-ice applications. A key requirement is to define a separability metric, as output from the model, which accords with a visual interpretation of whether a floe or lead can be successfully separated from its background. This linking of the model output with a visual interpretation is important because in practice the majority of ice analysis in operational ice centres is conducted by trained analysts, rather than using automatic algorithms.

In our study we consider two ice classes (first-year ice and multi-year ice) as well as leads. A lead is a linear fracture in the ice pack that is navigable by a ship. Leads generally appear as areas of low brightness in SAR images, because they contain “mirror-like” areas of relatively calm water or new ice. The model consists of the following steps:

- Look up the database of sea-ice properties: a predefined table of backscatter values for the ice types of interest is used, given the SAR parameters (radar frequency, polarisation and incidence angle).
- Specify the image parameters: the user inputs the required values of thermal noise, speckle, feature size and spatial resolution.
- Generate the simulated image: add thermal noise and single- or multi-look speckle.
- Calculate the separability metric based on Student’s t-test using the statistics of individual pixels from the feature and the background.
- Determine the value of the separability metric when features are just distinguishable from the background.

Initial investigations indicated that floe types or leads were distinguished for a separability metric of approximately 0.8. However, later results revealed a dependence on the size of the feature, and so the model was modified to use region statistics as in equation (1) above. As in the generic segmentation application above, the values from the t-statistic are lower when the region boundaries have to be estimated from the data (which is usually the case in practice).

Figure 5 shows an example of the predictions for lead detection in a first-year ice background (HH polarisation and IS3 incidence angle:  $26^{\circ} - 31^{\circ}$ ). The separability probability metric is presented as a function of lead width for four different thermal noise levels. As expected, Figure 5 shows that the leads become progressively less distinct for increased levels of thermal noise, so that finer spatial resolution is required in order to detect them.

The performance of the model has been assessed on example Envisat ASAR data from the Canadian Arctic, in Image (IM), Alternating Polarisation (AP) and Wide Swath (WS) modes. Degradations are introduced into the images (coarser spatial resolution or higher thermal noise) and the author (eOsphere) acting as an expert user then estimates when features of interest are visible. Figure 6 shows examples of the addition of thermal noise to WS data.

Plots such as Figure 5 provide a good match for the examples of floe discrimination which were studied here, but not for the cases with leads. In order to account for the behaviour of leads, the assumed number of pixels in the separability metric may be changed. This is equivalent to the approach in the generic segmentation where the ratio of t-values was computed for known boundaries and boundaries estimated from the SAR data. A possible reason for the distinctive behaviour for leads is the effect of edge pixels. Because leads are long and thin, a high proportion of pixels in the leads lie close to the boundary. When the effect of finite spatial resolution is taken into account, these pixels tend to be contaminated by the much brighter

signal from the surrounding ice. Image texture may also contribute, and it could also be important for ice floes. A further factor specific to this application is that it is not clear what size of background region should be used in the separability metric. Although the background area may be large, human interpretation tends to focus on scales comparable to features of interest and so it has been assumed that the background area is equal to the area of the feature being studied.

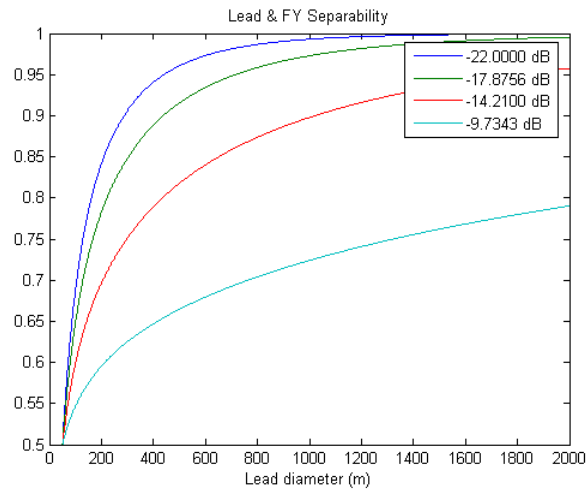


Figure 5 Lead detection: predicted probability of separation for four different noise levels.

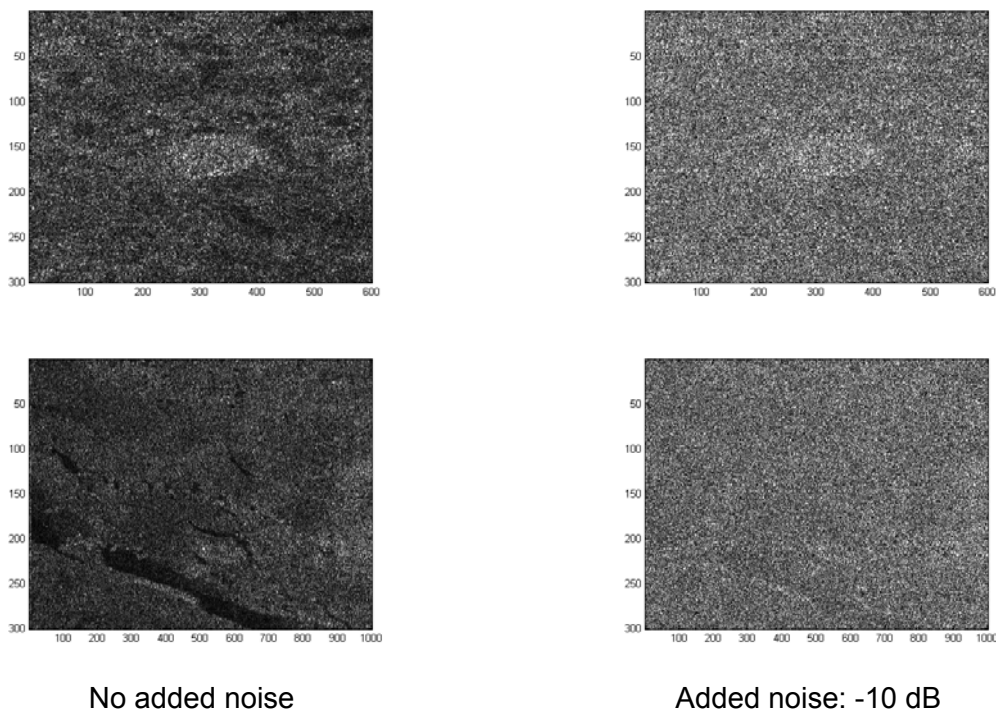


Figure 6 Floe (top) and lead (bottom) visibility reduced with addition of thermal noise to WS data: the axes are pixel numbers.

### **Conclusions and Recommendations**

This study has developed models to link the accuracy of geophysical parameters retrieved from SAR data to the values of SAR image quality and calibration parameters for a wide range of applications.

The main differences between the theoretical models and the practical results are as follows:

- The performance of retrieval algorithms which rely on segmentation can be predicted using models of uniform, speckled scenes, but the actual performance is worse because of the presence of image texture.
- Edge effects reduce the ability to detect small regions and long, thin regions such as leads in sea ice, because a relatively large fraction of the pixels in such regions is close to region boundary. Convolution contaminates these pixels with signal from the adjacent region. Thus the ability to detect small or long, thin regions of a given size becomes worse as the spatial resolution becomes coarser.

The following aspects may be recommended for further study.

- Develop further analysis to express different types of degradation in terms of the equivalent coarsening of spatial resolution. This is useful for the assessment of practical performance because the required spatial resolution is often the best established user requirement.
- Assessment of other applications: some applications such as ocean wave spectra may be robust against degradation because they do not rely on calibrated SAR data.
- Impact on higher-level products: e.g. meteorological models to resolve directional ambiguities in retrieved wind fields, and the derivation of the maps of sea-ice motion.
- Extension to interferometric SAR: examples include digital elevation maps, changes in height from differential interferometry, and surface ocean currents.
- Extension to the joint use of SAR data from different polarisations, and in both intensity and interferometry, e.g. for retrieval of forest biomass.
- Application to a biomass inversion scheme based on a Bayesian approach. This would model not only the approximate dependence of the radar backscatter on biomass, but also the spread of the actual data about the approximate model.
- Assessment of data quantisation, as this has implications for the data volumes which need to be transmitted and stored for particular studies.
- Enhancement of the ice type backscatter values used to populate the sea-ice database and extension of the sea-ice analysis to a wider range of test cases.

**END OF DOCUMENT**